Complex Ordering in Thin Films of Di- and Trifunctionalized Hexaalkoxytriphenylene Derivatives

Philippe Henderson,[⊥,||] Dierk Beyer,[†,||] Ulrich Jonas,[‡,||] Olaf Karthaus,[§,||] Helmut Ringsdorf,[||] Paul A. Heiney,[*,¶] Nicholas C. Maliszewskyj,[¶,#] Surya S. Ghosh,[¶] Oksana Y. Mindyuk,[¶] and Jack Y. Josefowicz[&]

Contribution from the Institut für Organische Chemie, Johannes Gutenberg Universität, 55099 Mainz, Germany, Department of Physics and Astronomy and Laboratory for Research on the Structure of Matter, University of Pennsylvania, Philadelphia, Pennsylvania 19104, and Department of Materials Science and Engineering, University of Pennsylvania, Philadelphia, Pennsylvania 19104

Received November 21, 1996[⊗]

Abstract: We have used pressure−area isotherms, X-ray diffraction, atomic force microscopy, and infrared dichroism to study Langmuir and Langmuir−Blodgett films of 2,3,6,7,10,11-hexaalkoxytriphenylenes which were selectively di- and trifunctionalized with C_nH_{2n}−OH groups at the 2,3-, 2,6-, 3,6-, and 3,6,10-positions. The bulk phase behavior of these compounds was also established with use of polarizing microscopy and differential scanning calorimetry. At the air−water interface, the hydroxy groups make contact with the water, and the Langmuir film stability is strongly correlated with proximity of the hydroxy groups on the molecule. Mixtures of 2,3- and 3,6-isomers display a dramatic increase of the liquid−crystalline mesophase temperature range compared to the pure compounds. The mixtures also have lower molecular areas at the air−water interface and produce thin films with a complex superlattice structure of disk tilts, showing for the first time the ability of triphenylene isomer alloys to self-organize.

1. Introduction

Recently, considerable attention has been devoted to ultrathin, layered structures of organic molecules. In particular, thin films of the disk-shaped molecules comprising discotic liquid crystals (LC's)[1] show promise for applications as pressure sensors,[2,3] anisotropic conductors,[4] and display devices,[5] due to their capability for self-organization in highly anisotropic structures at the air−water and air−solid interfaces.[6] Such films may be readily formed via the Langmuir−Blodgett (LB) technique, but this technique in general requires amphiphilic compounds.

The LC and thin-film properties of alkoxytriphenylenes and related compounds have been extensively studied.[7−9] Symmetrically-functionalized triphenylene derivatives are not manifestly amphiphilic, and do not tend to form highly stable Langmuir or LB films. For example, symmetric alkoxy derivatives have been shown to form Langmuir films,[10,11] while closely related alkylthio derivatives do not.[11] Triphenylene derivatives, as well as oligomers, for which the symmetry has been broken by functionalization with polar end groups display a higher degree of stability and readily form Langmuir and LB films;[12−14] the stability of the films and the orientation of the molecules relative to the water or solid surface depend sensitively on the chemical structure of the molecule.[11,15,16] In particular, the number of hydrophilic substituents, their positions on the triphenylene core, and their chemical natures are all tunable parameters that can influence the overall amphiphilic character.

The liquid crystalline 2,3,6,7,10,11-hexaalkoxytriphenylenes[7,8,17] generally form hexagonal columnar phases in the bulk, and were recently shown to be photoconductors with large and anisotropic charge carrier mobilities.[18,19] If these derivatives are partially functionalized with hydrophilic side chains (e.g., with OH or carboxylic groups), they form stable Langmuir monolayers at

* To whom correspondence should be addressed.
⊥ Present Address: Shell Research and Technology Centre Louvain-la-Neuve, B-1348 Ottignies-LLN, Belgium.
|| Institut für Organische Chemie, Johannes Gutenberg Universität.
† Present Address: Hoechst AG, BU Polymerisate/Alkylose, F+E PM I, 65926 Frankfurt am Main, Germany.
‡ Present Address: Lawrence Berkeley National Laboratory, Berkeley, CA 94720
§ Present Address: Research Institute for Electronic Science, Hokkaido University, Kita-Ku, Sapporo 060, Japan.
¶ Department of Physics and Astronomy and Laboratory for Research on the Structure of Matter, University of Pennsylvania.
# Present Address: Reactor Radiation Division, National Institute of Science and Technology, Gaithersburg, MD 20899.
& Department of Materials Science and Engineering, University of Pennsylvania. Present Address: ElectroStar, California Division, 8636 Aviation Blvd., Inglewood, CA 90301.
⊗ Abstract published in *Advance ACS Abstracts,* May 1, 1997.

(1) Chandrasekhar, S.; Ranganathan, G. S. *Rep. Prog. Phys.* **1990**, *53*, 57.
(2) Jin, S.; Tiefel, T. H.; Wolfe, R.; Sherwood, R. C.; Mottine, J. J., Jr. *Science* **1992**, *255*, 446.
(3) Schutt, J. D.; Batzel, D. A.; Sudiwala, R. V.; Rickert, S. E.; Kenney, M. E. *Langmuir* **1988**, *4*, 1240.
(4) Vincett, P. S.; Barlow, W. S. *Thin Solid Films* **1980**, *71*, 305.
(5) Zhu, Y.-M.; Lu, Z.-H.; Jia, X. B.; Wei, Q. H.; Xiao, D.; Wei, Y.; Wu., Z. H.; Hu, Z. L.; Xie, N. G. *Phys. Rev. Lett.* **1994**, *72*, 2573.
(6) Vincett, P. S.; Roberts, G. G. *Thin Solid Films* **1980**, *68*, 135.
(7) Tinh, N. H.; Dubois, J. C.; Malthete, J.; Destrade, C. *C. R. Acad. Sci. Paris* **1978**, *286*, 463.
(8) Destrade, C.; Mondon, M. C.; Malthete, J. *J. Phys.* **1979**, *4*, C3−17.
(9) Levelut, A. M. *J. Chim. Phys.* **1983**, *80*, 149.
(10) Albrecht, O.; Cumming, W.; Kreuder, W.; Laschewskyj, A.; Ringsdorf, H. *Colloid Polym. Sci.* **1986**, *264*, 659.
(11) Maliszewskyj, N. C.; Heiney, P. A.; Blasie, J. K.; McCauley, J. P.; Smith, A. B., III *J. Phys. II Fr.* **1992**, *2*, 75.
(12) Josefowicz, J. Y.; Maliszewskyj, N. C.; Idziak, S. H. J.; Heiney, P. A.; McCauley, J. P., Jr.; Smith, A. B., III *Science* **1993**, *260*, 323.
(13) Maliszewskyj, N. C.; Heiney, P. A.; Josefowicz, J. Y.; McCauley, J. P., Jr.; Smith, A. B., III *Science* **1994**, *264*, 77.
(14) Maliszewskyj, N. C.; Heiney, P. A.; Josefowicz, J. Y.; Plesnivy, T.; Ringsdorf, H.; Schuhmacher, P. *Langmuir* **1995**, *11*, 1666.
(15) Laschewsky, A. *Angew. Chem. Adv. Mater.* **1989**, *101*, 1606.
(16) Albrecht, O.; Cumming, W.; Kreuder, W.; Laschewsky, A.; Rinsdorf, H. *Colloid Polym. Sci.* **1986**, *264*, 659.
(17) Tinh, N. H.; Bernaud, M. C.; Destrade, C. *Mol. Cryst. Liq. Cryst.* **1981**, *65*, 307.
(18) Adam, D.; Closs, F.; Frey, T.; Funhoff, D.; Haarer, D.; Ringsdorf, H.; Schuhmacher, P.; Siemensmeyer, K. *Phys. Rev. Lett.* **1993**, *70*, 457.

S0002-7863(96)04036-X CCC: $14.00

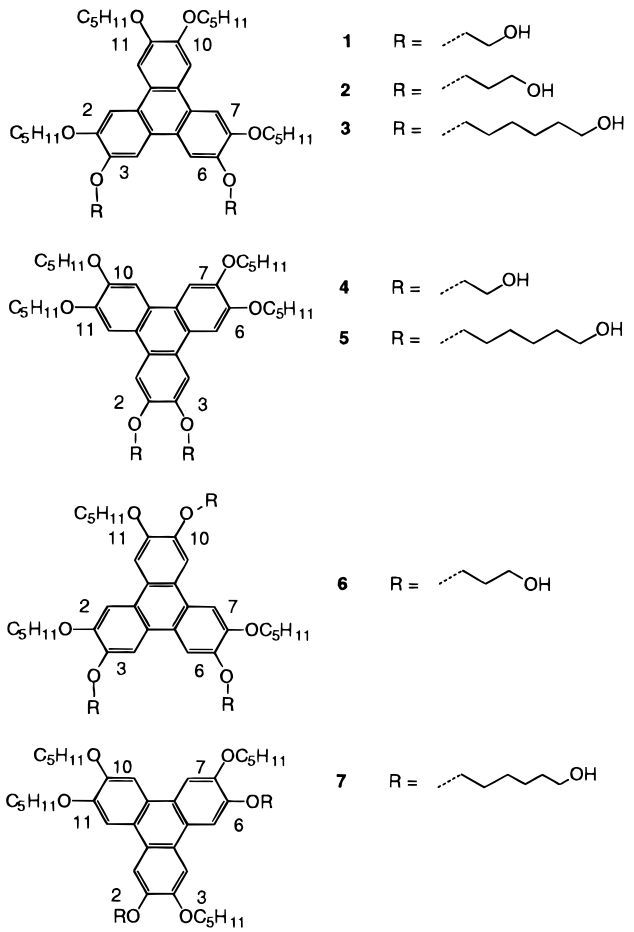

Figure 1. Compounds investigated in this study.

the air−water interface with a well-defined orientation of the molecules relative to the surface. Until recently, di- and trifunctionalized 2,3,6,7,10,11-hexaalkoxytriphenylenes could only be synthesized in a statistical approach by the so-called "trimerization route" in rather low yields.[17,20−24] With the development of new synthetic strategies toward functionalized triphenylenes,[25−28] pure isomers with two or more different side groups can be obtained in high yields. These molecules can be designed to enhance the stability of Langmuir or LB films, and in the future could also be modified to enhance their electronic, photophysical, or other properties.

In this paper[29] we investigate the physical properties of amphiphiles **1**−**7** (Figure 1), as well as of mixtures of **1** and **4**. **1**−**5** and **7** are triphenylenes which were difunctionalized with hydroxyalkyloxy chains of various lengths at the 2,3- and 3,6-positions, the other side chains being pentyloxy groups; **6** is a trifunctionalized triphenylene. In addition to determining the relative monolayer stability of these compounds, we find that mixtures of compounds **1** and **4** display an unusual capacity for self-organization in the bulk, and at both the air−water and air−solid interfaces.

The remainder of this paper is organized as follows: In Section II we provide the experimental details of our measurements. In Section II we discuss the bulk properties of compounds **1**−**7**, with particular reference to their thermodynamic phases. In Section IV we present spreading pressure measurements of **1**−**7** and mixtures of **1** and **4**. X-ray diffraction, atomic force microscopy, and infrared dichroism measurements are presented in Sections V and VI. We conclude with a speculative discussion (Section VII) of a structural model derived from our results.

II. Experimental Section

Synthesis and Physical Characterization. Compounds **2**−**4** were synthesized and purified as described in ref 27. Compound **1** was prepared according to the general procedure outlined in refs 27 and 28, with a 57% yield. Synthesis of and measurements on **5** have been described in refs 30 and 31. The samples of **6** that we studied were prepared by a "statistical" method,[32] but can also be prepared starting from **13b** in ref 27 following the experimental descriptions given in Scheme 9 of ref 27 (alkylating agent = $Br-(CH_2)_3-OH$). Compound **7** was prepared via a "statistical" method starting from **4a** in ref 33, as described in ref 32.

Calorimetry and optical microscopy measurements were carried out as described in ref 27. The phase behavior was measured on a Perkin Elmer Differential Scanning Calorimetry DSC 7, equipped with a Thermal Analysis Controller TAC 7/DX, a low temperature controller CCA 7, and a personal computer Epson EL Plus. The polarizing light microscope was a Leitz Ortholux II POL-BK equipped with a Mettler hot stage FP 52 and a hot stage controller FP 5.

II/*A* Isotherm Measurements. Spreading pressure (Π) versus area (A) isotherms of Langmuir films were measured at 20 °C on a Lauda FW 2 film balance (teflon, surface 930 cm^2), equipped with a Langmuir pressure pickup system. The spreading solutions were all approximately 10^{-4} M in concentration, CH_2Cl_2 was used as solvent, and a sample volume of 400 μL was spread for each measurement. The subphase was Milli Q water (resistivity *ca.* 18 MΩ cm). The molecular compression speed was between 1100 and 1800 $m^2\ s^{-1}\ mol^{-1}$, and except as explicitly noted below the spreading behavior did not change within these limits. The molecular compression speed was calculated from the surface area change divided by the measuring time and the sample quantity.

Formation of Langmuir−Blodgett Films. Lauda film balances were also employed for deposition of LB films. Monomolecular films at the air−water interface were transferred via the LB vertical dipping technique onto Si wafers. The AFM and XRD measurements employed Si wafers coated with a self-assembled monolayer of octadecyltrichlorosilane (OTS).[34] Hydrophilic Si surfaces for transmission infrared measurements were prepared by immersing the Si wafers in a solution of H_2SO_4 and H_2O_2 (9:1) for 4 h and then rinsing carefully with deionized, Millipore-filtered water and with methanol. The wafers were then dried in vacuum and used immediately for LB deposition. There was no measurable contact angle on these surfaces. Hydrophobic Si

(19) Adam, D.; Closs, F.; Frey, T.; Funhoff, D.; Haarer, D.; Ringsdorf, H.; Schuhmacher, P.; Siemensmeyer, K. *Ber. Bunsenges. Phys. Chem.* **1993**, *97*, 1366.
(20) Matheson, I. M.; Musgrave, O. C.; Webster, C. J. *J. Chem. Soc., Chem. Commun.* **1965**, *13*, 278.
(21) Boden, N.; Borner, R. C.; Bushby, R. J.; Cammidge, A. N.; Jesudason, M. V. *Liq. Cryst.* **1993**, *15*, 851.
(22) Piatelli, M.; Fattorusso, E.; Nicolaus, R. A.; Magno, S. *Tetrahedron* **1965**, *21*, 3229.
(23) Musgrave, O. C.; Webster, C. J. *J. Chem. Soc.* **1971**, *C*, 1397.
(24) Bechgaard, K.; Parker, V. D. *J. Am. Chem. Soc.* **1972**, *94*, 4749.
(25) Borner, R. C.; Jackson, R. F. W. *J. Chem. Soc., Chem. Commun.* **1994**, 845.
(26) Boden, N.; Bushby, R. J.; Cammidge, A. N. *J. Chem. Soc., Chem. Commun.* **1994**, 465.
(27) Closs, F.; Häussling, L.; Henderson, P.; Ringsdorf, H.; Schuhmacher, P. *J. Chem. Soc., Perkin Trans. 1* **1995**, 829.
(28) Henderson, P.; Ringsdorf, H.; Schuhmacher, P. *Liq. Cryst.* **1995**, *18*, 191.
(29) Some of the results of this paper have been previously presented as posters at the LB7 Conference, September 10−15, 1995, in Ancona, Italy, and the 16th International Liquid Crystal Conference, June 23−27, 1996, Kent, OH.
(30) Karthaus, O.; Ringsdorf, H.; Tsukruk, V. V.; Wendorff, J. H. *Langmuir* **1992**, *8*, 2279.
(31) Van der Auweraer, M.; Catry, C.; Chi, L.; Karthaus, O.; Knoll, W.; Ringsdorf, H.; Sawodny, M.; Urban, C. *Thin Solid Films* **1992**, *210/211*, 39.
(32) Karthaus, O. Ph.D. Thesis, Johannes Gutenberg Universität, Mainz, Germany, 1992.
(33) Kreuder, W.; Ringsdorf, H.; Tschirner, P. *Makromol. Chem. Rapid. Commun.* **1985**, *6*, 367.
(34) Sagiv, J. J. *J. Am. Chem. Soc.* **1980**, *102*, 92.

surfaces for transmission infrared measurements were prepared by treating the Si wafers as described above, following which they were exposed to a saturated atmosphere of hexamethyldisilazane at room temperature for 3 h. The slides were then baked at 120 °C for 1 h. The contact angle for the silanized silicon wafer was 94° (advancing) and 82° (receding).

Hydrophobic SiO_x surfaces for grazing-incidence FTIR were prepared with use of carefully cleaned glass slides, onto which 80 nm Ag and subsequently 14 nm SiO_x (oxygen pressure 2×10^{-4} mbar) were deposited with use of a Balzer BAE 250 evaporation apparatus. Directly after deposition these slides were exposed to a saturated atmosphere of hexamethyldisilazane at room temperature for 3 h, and then baked at 120 °C for 1 h. Contact angles on these samples were 93° (advancing) and 80° (receding).

Monolayer films on hydrophobic substrates were deposited on insertion of the substrate into the subphase for retrieval after the film had been removed. Bilayer and multilayer specimens were deposited on insertion and withdrawal of the substrate through the Langmuir film while keeping the surface pressure constant at all times. Transfer ratios were all on the order of 0.95. All specimens were placed in an inert atmosphere immediately after manufacture and could be stored indefinitely under conditions of controlled temperature and humidity.

X-ray Diffraction. X-ray studies were performed in the grazing incidence geometry with use of beamline X9B at the National Synchrotron Light Source at Brookhaven National Laboratory, as previously described.[14] A sagitally focussing Si(111) monochromator crystal selected a wavelength of 1.5405 Å. For initial experiments, two-dimensional diffraction patterns were collected by using Fuji image plates.[35] The specimen was oriented such that its angle with respect to the incoming beam was less than the critical angle for total external reflection. We define the [00*l*] crystallographic direction to coincide with the normal to the plane of the specimen, and [*h*00] and [0*k*0] to be mutually orthogonal vectors in the plane of the specimen. The instrumental resolution was approximately $\Delta q_l = 0.004$ Å^{-1} full-width at half-maximum (fwhm) along the [00*l*] direction and $\Delta q_h = 0.007$ Å^{-1} fwhm in the plane of the film. (We use the convention $q = 4\pi \sin(\theta/\lambda) = 2\pi/d$.) For more quantitative measurements the diffracted radiation was analyzed with use of a Ge(111) crystal and collected by using a scintillation counter, resulting in a tighter resolution $\Delta q = 0.0006$ Å^{-1} fwhm.

Atomic Force Microscopy. Atomic force images of the film surface were obtained on a Nanoscope III AFM[36] at 20 °C, with a 1 μm × 1 μm piezoelectric substrate translator having lateral and vertical resolution of less than 0.5 Å. The imaging experiments were performed with use of a silicon nitride tip in contact mode, with typical loads on the order of 10 nN. Images were recorded in several different areas on all samples. To determine that observed objects were not possible artifacts arising from AFM tip effects, the scan angle relative to the specimen was varied during the course of imaging. In all cases the orientation and scale of the observed structures were found to change in a manner consistent with the scan parameters. The instrument was calibrated before each measurement with a mica substrate. None of the images presented in this work have been filtered, frame-averaged, or otherwise altered in any way.

Infrared Reflection and Absorption. Grazing incidence and transmission FT-IR spectra were measured with a Nicolet 5DXC, equipped with an "Ever-Glo" light source and a nitrogen cooled HgCdTe narrow-band detector. Reflection measurements were performed using grazing incidence (80°) reflection on an FT80 apparatus. For each spectrum we measured 5000 scans at 8-cm^{-1} resolution.

Three different types of sample were employed for FTIR measurements on LB films of **1**, **4**, and their 1:1 mixture: (a) monolayers deposited on hydrophilic substrates for transmission measurements; (b) 20-layer films deposited on hydrophobic substrates for transmission measurements; and (c) 20-layer films deposited on hydrophobic substrates for reflectance measurements. Spectra were obtained for a region between 4000 and 650 cm^{-1} for the multilayers and between 1600 and 1200 cm^{-1} for the monolayers, respectively. For transmission measurements spectra were collected with the polarization parallel to the substrate plane and parallel (0°) or perpendicular (90°) to the dipping direction. The reflectance spectra were recorded with the IR beam parallel to the dipping direction and a polarization parallel (0°) to the substrate normal.

Background measurements for each silicon wafer were measured at the same polarization as for the corresponding sample measurement on an area uncoated with the organic film on the same wafer. Background measurements for the reflectance experiments were performed with use of an uncoated, hydrophobized slide as reference.

Table 1. Thermal Behavior of Compounds Studied in Bulk Form[a]

Compound	Isomer	R	Phases
1	3,6	$(CH_2)_2OH$	$K \underset{157°C}{\longleftrightarrow} I$
2	3,6	$(CH_2)_3OH$	$K \underset{87°C}{\longleftrightarrow} D_x \underset{99°C}{\longleftrightarrow} D_h \underset{118°C}{\longleftrightarrow} I$
3	3,6	$(CH_2)_6OH$	$K \underset{65°C}{\longrightarrow} (LC \underset{55°C}{\longleftarrow}) I$
4	2,3	$(CH_2)_2OH$	$K_1 \underset{113°C}{\longleftrightarrow} K_2 \underset{130°C}{\longleftrightarrow} LC \underset{139°C}{\longleftrightarrow} I$
5	2,3	$(CH_2)_6OH$	$K \underset{66°C}{\longrightarrow} (LC \underset{35°C}{\longleftarrow}) I$
6	3,6,10	$(CH_2)_3OH$	$K \underset{86°C}{\longleftrightarrow} D_x \underset{96°C}{\longleftrightarrow} D_h \underset{110°C}{\longleftrightarrow} I$
7	2,6	$(CH_2)_6OH$	$K_1 \underset{44°C}{\longleftrightarrow} K_2 \underset{49°C}{\longleftrightarrow} D_h \underset{67°C}{\longleftrightarrow} I$
1:1 **1** + **4**		$(CH_2)_2OH$	$LC \underset{147°C}{\longleftrightarrow} I$

[a] K = crystal, D_h = hexagonal columnar phase, D_x = columnar phase of unknown symmetry, LC = unknown liquid crystal, I = isotropic liquid. The bottom entry shows the phase behavior for a 1:1 mixture of **1** and **4**.

III. Bulk Properties

The phase behavior of compounds **1**−**7** was established by using polarizing microscopy and differential scanning calorimetry (DSC). Our results are summarized in Table 1. Note first that, while the length of the functionalized chains has a strong influence on the stability of LC phases, for pure compounds the *position* of the functionalized chain has only a minor effect. A two-carbon chain is too short for LC formation, as demonstrated by the fact that **1** has no LC phase and **4** has only a LC phase over a very narrow temperature range. Compounds having three-carbon chains have a rich phase structure, as demonstrated by **2** and **6**, which have both a hexagonal-columnar D_h phase and an additional highly ordered mesophase of unknown structure. Finally, a six-carbon spacer is too long; both **3** and **5** show only monotropic LC phases.

Additionally, we examined the phase behavior of a 1:1 mixture of **1** and **4**. The results were dramatic: the mixture is clearly seen by polarizing microscopy and calorimetry to be liquid crystalline down to below 0 °C, even though **1** does not have an LC phase and **4** only has a mesophase over a very limited temperature range. While it has long been known that the LC temperature range of benzene-derived,[37] triphenylene-derived,[8] and other discotic LC phases can be greatly increased by mixing two different compounds, we have now demonstrated for the first time an increase in the temperature range of an LC mesophase by mixing two isomers of the same triphenylene derivative. Since both isomers are amphiphiles, we were motivated by these preliminary results to study the effect of mixing them on the properties of Langmuir and LB films.

IV. Formation and Characterization of Langmuir and Langmuir−Blodgett Films

Spreading pressure (Π) versus molecular area (A) isotherms measured at room temperature for Langmuir films of compounds

(35) *Fuji image plates*, Fuji Photo Film Co., Ltd.: 26-30 Nishiazabu 2-Chome, Minato-Ku, Tokyo 106, Japan.

(36) Digital Instruments: Santa Barbara, CA 93117.

(37) Chandrasekhar, S. *Mol. Cryst. Liq. Cryst.* **1981**, *63*, 171.

(38) Schwartz, D. K.; Garnaes, J.; Viswanathan, R.; Zasadzinski, J. A. N. *Science* **1992**, *257*, 508.

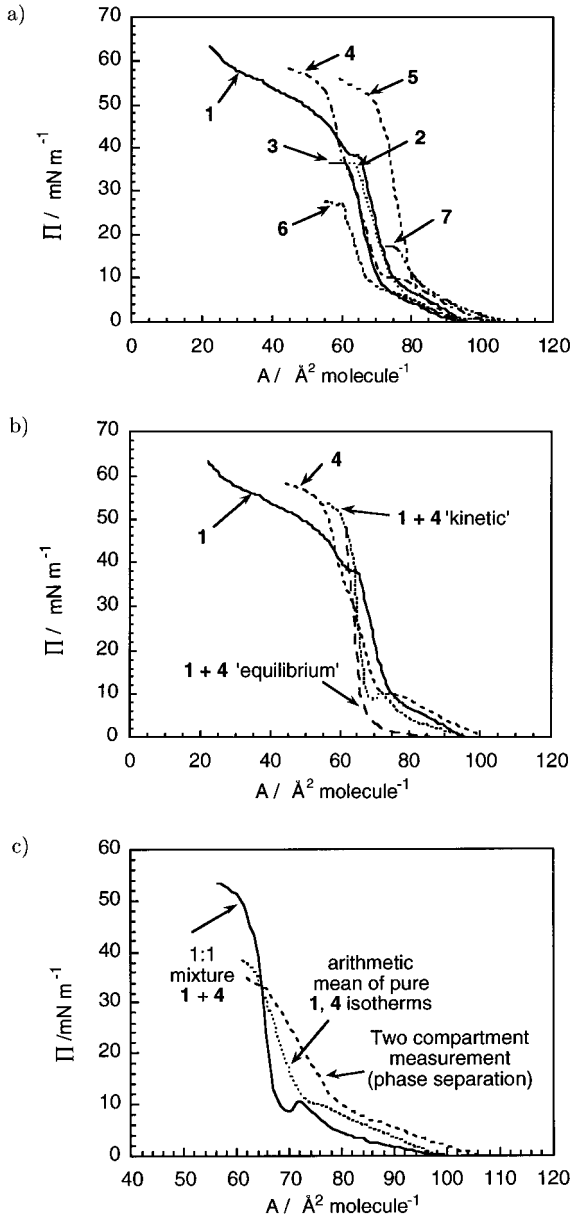

Figure 2. (a) Spreading pressure Π versus molecular area *A* isotherms for Langmuir films of compounds **1**−**7**. (b) Isotherms for **1**, **4**, and a 1:1 mixture of **1** and **4** measured under "kinetic" conditions (*ca.* 1100 m^2 s^{-1} mol^{-1}), and an isotherm of the mixture measured under quasiequilibrium conditions (slow compression over a period of *ca.* 2 h). (c) "Kinetic" isotherm of the 1:1 mixture of **1** and **4** compared with isotherms of the two compounds that were initially prepared in two separate compartments, and the arithmetic mean of the pure compound isotherms, as described in the text.

1−**7** are shown in Figure 2a. It is observed that when the attractive forces between the mesogens and the liquid subphase are weak and there are strong attractive interactions between the π electron systems on adjacent disks, the molecules tend to pack cofacially, such that the disk is oriented "edge-on" to the water surface. This is the usual case for triphenylene derivatives,[11−14] and it is the case here. All the compounds studied have molecular surface areas in the range 70−80 $Å^2$ $molecule^{-1}$. Compound **4** has a substantially smaller area (∼70 $Å^2$ $molecule^{-1}$) than **5** (∼80 $Å^2$ $molecule^{-1}$), for reasons that are unclear. Significantly, the monolayers of the 3,6 compounds **1**, **2**, and **3** are all less stable (collapse pressure ∼35 mN m^{-1}) than those of the 2,3 compounds **4** and **5** (collapse pressure ∼50 mN m^{-1}), in the sense that the collapse takes place at lower spreading pressures. Indeed, the difunctionalized compound **7**, carrying two OH groups far from each other (and carrying at least one pentyl chain between the hydrophyilc groups), is even less stable, collapsing at ∼18 mN m^{-1}.[32]

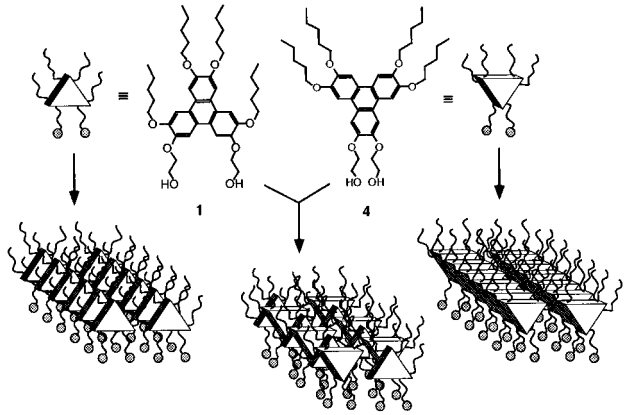

Figure 3. Schematic diagram of molecular order in Langmuir films of a 1:1 mixture of **1** and **4**. Each molecule tends to lie with its hydroxy groups adjacent to the water, and can be represented schematically by a triangle. When the compounds are mixed they can pack more efficiently by alternating up and down triangles.

Compound **6** presents a different situation: There is more than one possible "edge-on" orientation, which allows a more dense packing to be obtained by the juxtaposition of molecules in different orientations. However, this also introduces a new type of irregularity in the film, which may explain the relatively low collapse pressure (∼28 mN m^{-1}). The collapse pressure of **6** is thus lower than that of "good" amphiphiles, but larger than that of **7** for which the OH groups are *always* far from each other. All of these results are all consistent with the physically plausible hypothesis that the hydroxy groups make contact with the water, and that Langmuir films composed of molecules with hydroxy groups in close proximity to each other are more stable than films composed of molecules with well-separated hydroxy groups.

Figure 2b re-displays the isotherms of **1** and **4**, together with the isotherm for a 1:1 mixture of **1** and **4** at fast "kinetic" compression (ca. 1100 m^2 s^{-1} mol^{-1}) and slow "equilibrium" compression. Note that the surface area per molecule of the mixture is significantly smaller than the specific area for either **1** or **4** individually. We can understand this effect by examining the schematic diagram in Figure 3. Considering the shape of the molecules, we can think of **1** and **4** as being respectively "right-side-up" and "up-side-down" triangles. With the requirement that the hydroxy groups face the water, each compound individually will self-organize in such a way that alkyl tails in adjacent molecules are next to each other. When the compounds are mixed, we suggest that they are organized with up and down triangles alternating, leading to a much more efficient packing of alkyl tails and a smaller area per molecule. Recent glancing-angle X-ray diffraction measurements on Langmuir films of **1**, **4**, and their 1:1 mixture[39] confirm that there is a structural reorganization in the mixture, but suggest that the structure is more complicated than a simple alternation of up and down triangles, with more than one phase being present.

If the mixed film was compressed relatively rapidly (*ca.* 1100 m^2 s^{-1} mol^{-1}), the pressure at any given area was larger than that for slow compression. We will refer to this as "kinetic" compression. If the film was compressed rapidly and then stopped at some point on the compression curve, we observed a slow relaxation toward a lower pressure for any given

(39) Gidalevitz, D.; Mindyuk, O.; Heiney, P.; Ocko, B.; Henderson, P.; Ringsdorf, H.; Boden, N.; Strzalka, J.; McCauley, J. P.; Smith, A. B. Unpublished.

molecular area. In order to measure the "equilibrium" molecular area as a function of spreading pressure, we observed that it was necessary to compress the mixed film very slowly, over a period of at least 2 h, i.e., 250 $m^2\ s^{-1}\ mol^{-1}$. The results of such a slow compression on the **1** + **4** mixture are also shown in Figure 2b. The non-equilibrium maximum has disappeared, indicating that this was a purely kinetic effect. It would appear that considerable time is required for the two compounds to "recognize" each other and to self-organize into a dense alternating structure. We believe that the inflection point at ~10 mN m^{-1} observed under rapid compression was the point where the film rearranged itself to reduce its internal pressure, rather than being a true "collapse point". This hypothesis is supported by the observation that the pressure continued to rise as the film was further compressed. Once formed, however, the film was quite stable; an isotherm of the mixture had the same form even after spending a night at room temperature, indicating that there was no large-scale demixing. The decompression curve was always quite similar to the "equilibrium" curve. By contrast, 47 mN m^{-1} is a true collapse point, above which the decompression curve did not follow the compression curve.

Although the isotherms depended on compression rate, at any given compression rate they were highly reproducible, even when measured on different troughs in different laboratories.

When the isotherm was measured at 33 °C instead of room temperature, the molecular areas resembled those of **1** or **4** individually, indicating that either the triangles were no longer alternating or that it is less probable that the hydroxy groups on each molecule are adjacent to the water. When the isotherm was measured at 5 °C, the molecular areas were even lower than at room temperature, and the film was stable up to more than 55 mN m^{-1}, as one might expect for pre-formed crystallites floating on the water surface.

To verify our hypothesis that the reduced molecular area in the 1:1 mixture of **1** and **4** was a consequence of microscopic mixing of the two compounds, we made a measurement in which the two pure compounds were deposited on the water surface in two separated compartments. The barrier separating them was then removed before the combined film was compressed. In this way, we recorded a $\Pi-A$ curve for a mixture that was constrained to be phase separated. The kinetic isotherm recorded in this case (Figure 2c) was quite different from that obtained when spreading the mixture. It was in good qualitative agreement, however, with the results of a direct arithmetic average of the two kinetic isotherms recorded for the pure compounds **1** and **4**, i.e., a curve in which we plot the average of the recorded spreading pressures for **1** and **4** at each area (Figure 2c).

All compounds could be transferred to solid substrates (glasses, quartz, mica, or silicon) via the LB technique. We found that at most one layer could be transferred onto hydrophilic surfaces, with the plate coming out of the water during the transfer. It was possible to prepare multilayers (up to 40 or more layers) on hydrophobic surfaces. In this case, the transfer took place while dipping in *and* out (Y-type transfer).

V. X-ray Diffraction and Atomic Force Microscopy

We used grazing-incidence X-ray diffraction (GXRD) to study a 20-layer LB film of **1** (Figure 4), a 30-layer LB film of **4**, and a 20-layer LB film of their 1:1 mixture (Figure 5). These patterns were collected on Fuji imaging plates. The [00*l*] direction corresponds to "meridional" scattering with momentum transfer q_{00l} perpendicular to the surface, which measures the Fourier transform of the variation of charge density from layer to layer, $\rho(z)$. The [*h*00] direction corresponds to purely in-plane, or equatorial scattering, measuring the Fourier transform of $\rho(x,y)$. Off-axis scattering that is neither along the equator nor along the meridian probes correlations from layer to layer. For each sample, patterns were measured both with the beam essentially parallel to the dipping direction, corresponding to $\vec{q}$ perpendicular to the dipping direction, and with the beam perpendicular to the dipping direction, corresponding to $\vec{q}$ parallel to the dipping direction.

All patterns collected with the incident beam parallel to the dipping direction show the same general qualitative features:

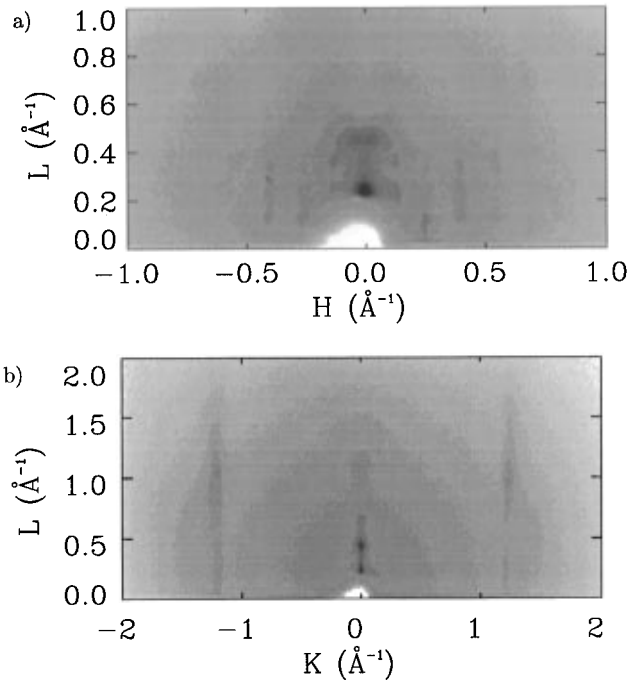

Figure 4. X-ray diffraction patterns from a 20-layer LB film of **1**: (a) incident beam parallel to the dipping direction; (b) Incident beam perpendicular to the dipping direction.

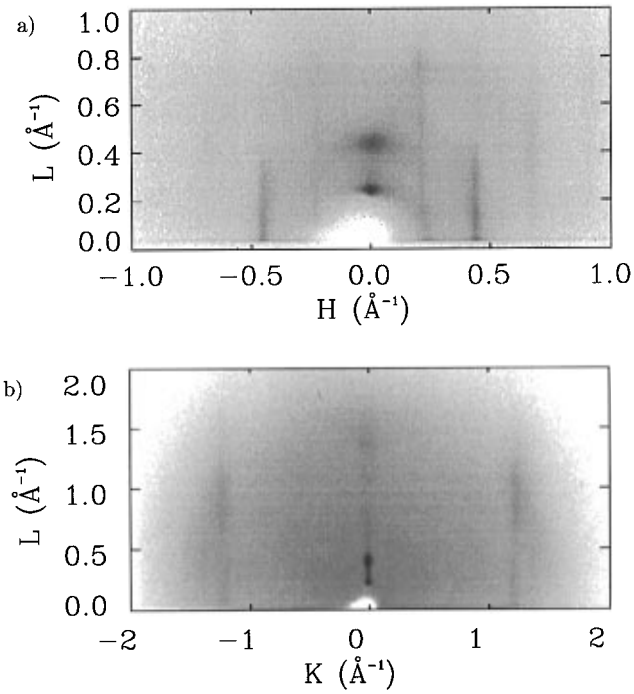

Figure 5. X-ray diffraction patterns from a 20-layer LB film of a 1:1 mixture of **1** and **4**: (a) incident beam parallel to the dipping direction; and (b) incident beam perpendicular to the dipping direction.

Table 2. Summary of X-ray Diffraction Results on a 20-Layer LB Film of **1**, a 30-Layer LB Film of **4**, and a 20-Layer LB Film of a 1:1 Mixture of the Two Compounds[a]

compd	d_{001} (Å)	d_{100} (Å)	ξ_{100} (Å)	d_{010} (Å)	ξ_{010} (Å)	χ (deg)
1	27.2 ± 0.1	45.8 ± 2.4	143 ± 8	4.90 ± 0.03	30 ± 3	38.8 ± 1.2
4	26.6 ± 0.1	32.4 ± 1.2	48 ± 8	4.72 ± 0.03	23 ± 2	38.3 ± 1.5
1:1 **1** + **4**	29.7 ± 0.1	27.5 ± 0.9	132 ± 7	4.89 ± 0.03	29 ± 3	37.9 ± 1.7

[a] d_{001} is the layer thickness, determined by the diffraction along the meridional direction. d_{100} and d_{010} are the repeat distances perpendicular to and parallel to the dipping direction, respectively, determined by the positions of Bragg rods at low angle (100) and diffuse scattering at high angle (010). ξ_{100} and ξ_{010} are the corresponding correlation lengths. χ measures the angle by which the maximum of the (010) peak is displaced from the equator; this displacement in general arises from a non-zero tilt of the triphenylene molecules relative to the layer normal.

a set of well-defined spots along the meridian, which correspond to the well-known Kiessig fringes together with 00*l* Bragg peaks, and a set of low-angle "Bragg rods" along the equator, which arise from intralayer order. Modulation or structure within each Bragg rod arises from both interlayer correlations and the structure factors of molecules within a single layer. By contrast, patterns collected with the incident beam perpendicular to the dipping direction show in general the meridional Bragg peaks and wide-angle diffuse scattering along the equator.

These observations are all indicative of the formation of a layered, columnar structure, similar to that of a bulk columnar phase, as previously observed in LB films of triphenylene derivatives.[12,13] Each layer consists of a set of columns, which are approximately aligned along the dipping direction. Within each column, the molecules are approximately "edge-on" to the surface. The 00*l* Bragg peaks measure the layer thickness. The multiple orders of *h*00 Bragg rods seen in the "parallel" patterns measure the intercolumnar spacing, whereas the wide-angle diffuse 0*k*0 scattering observed in the "perpendicular" patterns arises from a combination of tail disorder and intracolumnar order. We note that the intensity within the Bragg rods is in general maximized at a point off the equator. This provides a preliminary indication that the molecules are tilted within each column, resulting in an off-equatorial maximum in the structure factor.

Scattered intensities were extracted from the two-dimensional detector data via strip integration. Least-squares fits were then performed by using a Gaussian line shape for the intensity,

$$I(q) = A \exp(-(q - q_{hkl})^2/\Delta_{hkl}^2) \qquad (1)$$

The peak widths Δ_{h00} of the (*h*00) Bragg rods were found to increase linearly with momentum transfer q_{h00}, following the form

$$\Delta_{h00} = \Delta_1 + q_{h00}\Delta_2 \qquad (2)$$

The constant term Δ_1 is related by the correlation lengths quoted in Table 2 by $\xi_{100} = 2/\Delta_1$. From the magnitude of the linear term, $q_{h00}\Delta_2$, we infer that these films exhibit ∼6−9% paracrystalline disorder or strain within each layer. The d-spacings are then obtained from $d_{hkl} = 2\pi/q_{hkl}$. The correlation length along the "short" in-plane direction was obtained from the peak width by $\xi_{010} = 2/\Delta_{010}$.

A quantitative summary of our GXRD results is provided in Table 2. d_{001} is the layer thickness, which was determined by measuring Bragg peaks along the meridional direction. These distances are seen to be typically 27−30 Å, larger than the 18-Å size of the constituent disks but smaller than the 36−Å thickness one would calculate for a bilayer composed of two columns. A 27−Å distance can be understood as being the thickness of a *bilayer* of molecules with alternating tilts of ∼40°. The molecular tilt reduces the thickness of each layer from 18 Å to 18 Å cos(40°) ≈ 14 Å, and the alternation of tilts ensures that the repeat unit measured by GXRD is a bilayer rather than a monolayer. (It is also possible that the odd-order peaks are significantly reduced by the molecular structure factor and that all molecules tilt the same direction.)

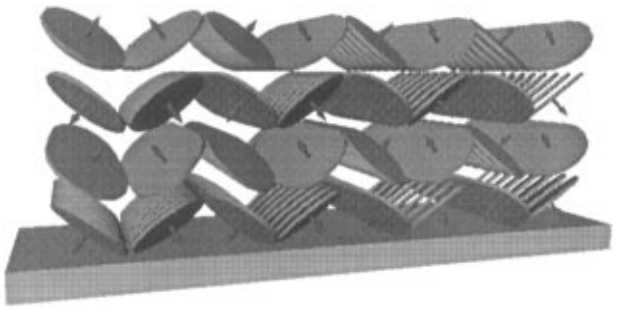

Figure 6. Schematic diagram of the hypothesized structure of columnar multilayer LB films of **4** and the 1:1 mixture of **1** + **4**. The disks are assumed to be tilted with respect to both the layer normal and the column axis, with an alternation of tilts both parallel and perpendicular to the surface normal. (Compound **1** forms a three-column repeat unit, most likely corresponding to three different tilt directions.)

The values of d_{010} quoted in Table 2 are the repeat distances parallel to the dipping direction, determined by the positions of diffuse maxima at high angle. The 4.8−Å repeat unit along the [0*k*0] direction and the relatively short 12−31 Å correlation lengths correspond to short-range intracolumnar order with molecules separated by the van der Waals thickness of the disks, as is commonly seen in bulk columnar phases of triphenylene compounds. The fact that the 4.8−Å feature is actually maximum at ∼38° off the equator is again consistent with a 40° tilt of the molecules. However, the very gradual variation of intensity along the [00*l*] direction, with a correlation length of only ∼4 Å, indicates that there are only short-range interlayer positional correlations.

The values of d_{100} quoted in Table 2 are the repeat distances perpendicular to the dipping direction, determined from the positions of low-angle Bragg rods. The distances quoted are much larger than the 18−20 Å expected for columns of triphenylene disks. This indicates a higher degree of structural complexity than is normally seen in LB films of triphenylene derivatives. One possible model involves rotations, or tilts, of the molecules about two axes, first by an angle $\alpha \approx 40°$ about an axis in the layer plan and perpendicular to the columns, and then by an angle $\beta \approx 40°$ about an axis perpendicular to the layers. In this case, the structures of **4** and the mixture can be explained by a simple alternation of rotations, yielding the desired spacing, as shown schematically in Figure 6. For compound **1**, the 46 Å spacing would require a three-column repeat unit.

As discussed above, the anisotropy manifested in the images with the beam parallel and perpendicular to the dipping direction indicates that the columns are oriented roughly parallel to the dipping direction. Quantitative measurements of the orienta-

(40) Evans-Lutterodt, K. W.; Isaacs, E. R.; Platzman, P. M.; Vandenberg, J. M.; Imperatori, P.; MacDowell, A. A.; Bean, J. C.; Ketelsen, L. C. Unpublished.

tional dependence of the Bragg rods were performed by rotating the specimen an angle ϕ about the substrate normal while maintaining the diffraction condition for the 100 Bragg rod. For this purpose the diffracted radiation was measured with use of a Ge analyzer and a scintillation detector in place of the imaging plate. For **1**, the variation of intensity with ϕ was best fit by using a Gaussian with full-width at half-maximum (fwhm) of 88°, while for **4**, the fitted fwhm is 22°.

Finally, we note an unexpected feature of the data. The 002 reflection of the diffraction pattern of **1** measured with the beam parallel to the dipping direction (Figure 4a) manifests an unusual splitting not observed in the orthogonal direction. Such a feature is sometimes associated with faceting of a crystal face. We are confident that in our measurements this effect is not due to a crack or rupture in the substrate. The most likely origin of the splitting is some type of periodic modulation in the height of the top layer, indicative of the onset of faceting.[41]

For AFM measurements, LB films were prepared on Si wafers coated with OTS. We were able to obtain high-quality images of multilayer films of **4** and the **1** + **4** mixture. In a 4-layer film of **4** we observe a striped structure with a 15.7(5)-Å intercolumnar spacing. This is only slightly smaller than the estimated 18-Å diameter of the disks, and is consistent with a structure in which the molecules are organized into columns with a small intracolumnar tilt, as discussed above. The columns were roughly oriented along the dipping direction. In a 6-layer film of a 1:1 mixture of **1** and **4** we noted the presence of two distinct length scales, on the order of 4 and 8 Å, respectively, roughly at right angles to each other. The 4−Å spacing is slightly smaller than an estimated intracolumnar disk spacing, but the 8-Å spacing is less than half the estimated diameter of one molecule. Such a distance could represent a column thickness if the disks were tilted within the columns by more than 60°, although this seems unlikely; more work will be required to clarify this structure.

VI. Infrared Dichroism

As discussed above, only monolayer LB films could be deposited on hydrophilic substrates. Transmission FTIR spectra from monolayer LB films on hydrophilic substrates were collected with the polarization at 90° (perpendicular to the dipping direction) and 0° (parallel to the dipping direction), as shown in Figure 7.

A monolayer of **1** shows little dichroism within the error margins of the measurement, while monolayers of **4** and the 1:1 mixture of **1** and **4** show a rather strong dichroism in polarized transmission FTIR, indicating a well-ordered monolayer on the hydrophilic silicon support. The FTIR results are consistent with a columnar orientation for both monolayers of **4** and of the 1:1 mixture of **1** and **4**, whereas no order can be determined in a monolayer of **1**. Transmission FTIR measurements of 20-layer films deposited on hydrophobized silicon substrates were also performed at 0° and 90° polarization, as shown in Figure 8. Reflection FTIR measurements were performed only at 0° polarization. The IR absorbance bands were assigned to the vibrations of molecular fragments according to the literature.[42−45] IR-dichroism measurements of the multilayers of pure compounds **1** and **4** and their 1:1 mixture were evaluated and are summarized in Table 3. None of the investigated multilayers show a strong dichroism in FTIR, and the dichroic ratios observed in each sample are very similar.

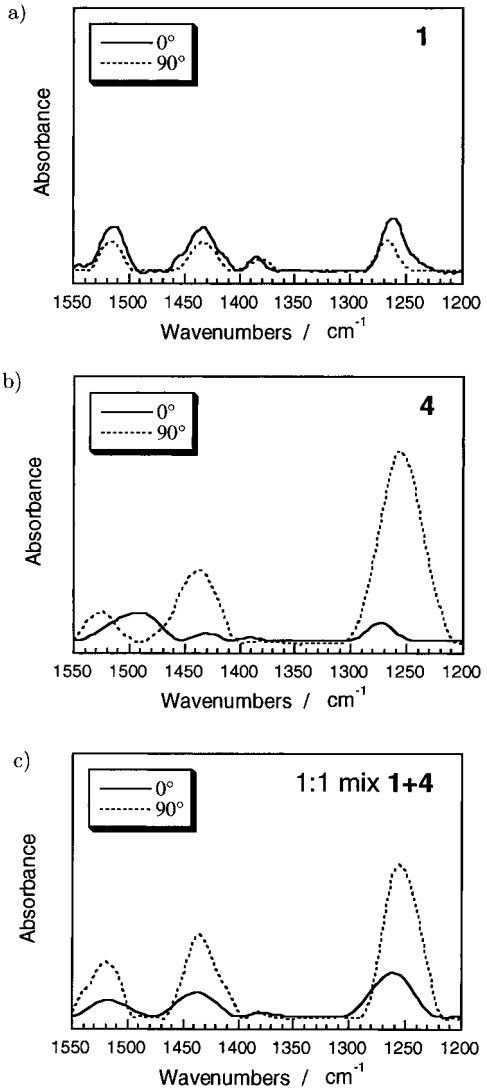

Figure 7. Transmission infrared spectra of LB monolayers of compounds **1** (a), **4** (b), and their 1:1 mixture (c). Absorbances are given in arbitrary units.

There are several possible explanations for the low dichroism in monolayer films of **1** compared to **4** and the mixture. It could arise from a structure in which the molecules lie flat on the surface, but this seems unlikely, given the measured areas at the air−water interface and the GXRD results presented in the previous section. It could also arise from a columnar structure with a nearly random distribution of columnar orientations. This interpretation is supported by the GXRD ϕ-rotation measurements on *multilayer* films of **1**, which showed a wide, if not isotropic, distribution of columnar orientations, and AFM measurements on multilayers of **1** which were essentially featureless, as characteristic of a highly disordered structure. Finally, a weak dichroism could be the result of a highly *ordered* structure with many different orientations of different molecules, such as that shown in Figure 6. It is possible, for example, that the hydrophilic groups in **1** are too far apart to act as one hydrophilic moiety of the molecule, and therefore induce a disorder or a strong tilt in the perpendicular direction (i.e., 45°)

(41) The diffraction intensity for a sinusoidally modulated surface has recently been analyzed,[40] and consists of a set of parallel satellite Bragg rods, separated by $n\,q$, where q is the periodicity of the modulation, and with intensities in the q_z direction modulated by the nth Bessel function.

(42) Kruk, G.; Kocot, A.; Wrzalik, R.; Vij, J. K.; Karthaus, O.; Ringsdorf, H. *Liq. Cryst.* **1993**, *14*, 807.

(43) Kruk, G.; Vij, J. K.; Karthaus, O.; Ringsdorf, H. *Supramol. Sci.* **1995**, *2*, 51.

(44) Vandeyvyver, M.; Albouy, P.-A.; Mingotaud, C.; Perez, J.; Barraud, A.; Karthaus, O.; Ringsdorf, H. *Langmuir* **1993**, *9*, 1561.

(45) Detailed assignments for modes are given in the following: Jonas, U. Ph.D. Thesis, Johannes Gutenberg Universität, 1996.

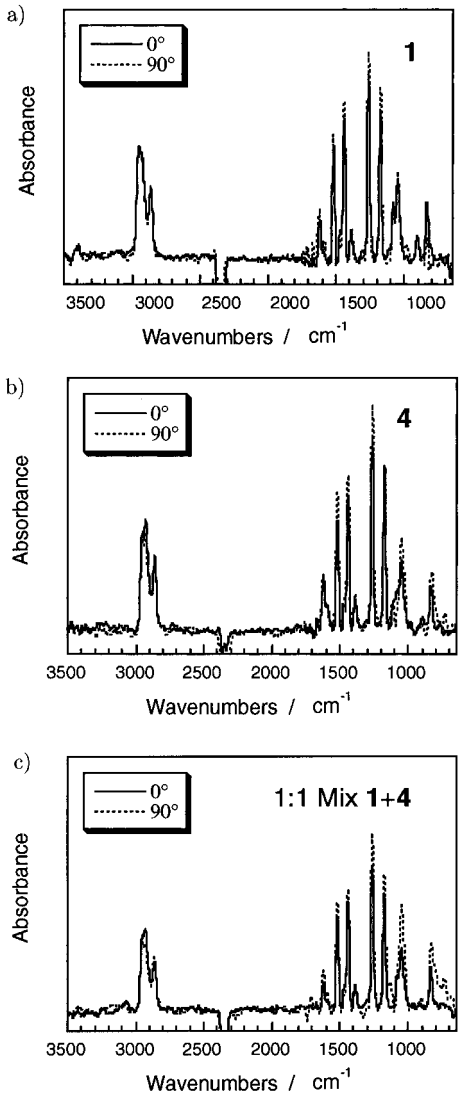

Figure 8. Transmission infrared spectra of 20-layer LB films of compounds **1** (a), **4** (b), and their 1:1 mixture (c). Absorbances are given in arbitrary units. The negative absorptions around 2350 cm^{-1} arise from CO_2 in the measuring cell atmosphere.

toward the dipping direction in the prepared monolayer, whereas the 2,3-functionalization in **4** leads to nicely organized monolayers on a hydrophilic support. The most likely scenario combines a complex local order with a high degree of orientational disorder of the columns. The low IR dichroism measured for multilayers of **1** and the **1** + **4** mixture is again consistent with a broad distribution of columnar orientations, a complex local structure incorporating many different tilt angles, or a combination of the two.

The IR-dichroism measurements on a 20-layer film of **4** deposited on a hydrophobized silicon wafer yield a dichroic ratio similar to that obtained for the multilayer structure of **1**. Nevertheless, the GXRD data indicate a much stronger columnar orientation along the dipping direction for **4** than **1**. A 22° distribution of column directions about the dipping direction cannot account for the low measured IR-dichroic ratios. Therefore, these data in combination with the GXRD measurements support the alternating tilt structure shown in Figure 6 and discussed in Section V, which would lead to a significantly lowered dichroic ratio in FTIR.

Intensities of transmission and reflectance data are not directly comparable, due to different path lengths of the IR beam in the sample. However, an approximate comparison could be made by using the simple assumption that the alkyl chains in the sample are highly disordered, so that the orientations of the transition dipole moments of the C−H vibrations $\nu_{C-H} = 2863-2960$ cm^{-1} are isotropically distributed in space. Then, all peaks in the spectra can be normalized in intensity by dividing by the average of the C−H vibration intensities. The results of such a calculation are given in Table III. The orientation of the transition dipole moments in space can then be reconstructed from the dichroism ratios. Using these assumptions, we obtain in-plane tilt angles $\chi_{||}$ of 40° for **1**, 38° for **4**, and 37° for the 1:1 mixture. The tilt angles along the layer normal, χ_{perp}, were calculated to be 25° (**1**), 33° (**4**), and 28° (mixture). Of course, these values provide only a rough approximation due to the averaging over columnar and molecular orientation distributions.

Table 3. Summary of Infrared Dichroism Results from LB Multilayers (**1**: 20 Layers; **4**: 30 Layers; mix: 20 Layers)[a]

wavelength (cm^{-1})	orientation of $\vec{\mu}$ to core	**1**		**4**		mix	
		I_{90}/I_0	Ref/I_0	I_{90}/I_0	Ref/I_0	I_{90}/I_0	Ref/I_0
2956	isotropic	0.988	1.069	1.026	1.123	0.994	1.136
2933	isotropic	1.001	0.953	0.940	0.892	0.884	0.874
2863	isotropic	1.017	0.962	1.056	0.999	1.207	1.001
1618	parallel	1.326	2.120	1.310	1.148	1.706	2.133
1520	parallel	1.095	2.618	1.398	2.074	1.318	2.330
1438	parallel	1.143	1.767	1.272	1.449	1.259	1.632
1390	parallel	1.239	2.278	1.318	1.833	1.110	1.937
1267	parallel	1.156	2.256	1.304	1.819	1.381	2.344
1175	parallel	1.167	1.599	1.106	1.091	1.322	1.144
1083	independent	0.825	1.128	0.744	1.882	1.353	1.747
1053		1.115	1.871	1.479	1.686	1.892	1.669
906	perpendicular	1.017	1.459	0.366	1.892	8.511	11.876
838	perpendicular	0.368	0.467	1.472	0.714	1.777	0.454

[a] The first column indicates the wavenumber and the second column the orientation of the transition dipole moment $\vec{\mu}$ in relation to the triphenylene core: "parallel" refers to $\vec{\mu}$ in the plane of the core, and "perpendicular" refers to $\vec{\mu}$ normal to the plane of the core.[45] For the 1053-cm^{-1} peak the dipole moment orientation depends on the orientations of the alkyl chains. For each wavelength and each sample (**1**, **4**, or their 1:1 mixture), I_{90}/I_0 indicates the normalized absorbance in 90° polarization divided by the normalized 0° polarization (both in transmission), while Ref/I_0 indicates the normalized absorbance in the reflection geometry (with 0° orientation relative to the dipping direction) divided by the 0°-polarization normalized transmitted intensity.

VII. Discussion and Summary

We have shown that the new synthetic strategies for di- and trifunctionalized 2,3,6,7,10,11-hexaalkoxytriphenylenes in high yields provide molecules with qualitatively new properties. Furthermore, new effects are seen when two isomers of a triphenylene derivative are mixed. Equimolar mixtures of **1** + **4** display very different bulk phase behavior from either **1** or **4**, i.e., a dramatic increase of the mesophase temperature range. These mixtures also have lower molecular areas at the air−water interface and produce thin films with different complex structures, showing for the first time the ability of triphenylene isomer blends to self-organize. In our model for the Langmuir films, presented schematically in Figure 3, the molecular areas are reduced by the juxtaposition of neighboring molecules with different orientations. Our picture of the thin-film structure is still incomplete, but it is clear that the degree of columnar order is substantially different in **1** and **4**, and it seems likely that higher-order structures are generated via alternations of molecular tilts.

We speculate that the enhancement of the bulk mesophase range in the **1** + **4** mixture may arise from an alternating superlattice of the **1** and **4** isomers, in a manner very similar to that shown for monolayers in Figure 3. Direct structural measurements of the intracolumnar orientational order in the disordered columnar phases of triphenylene-based discotic LC's are difficult, but the closely related crystalline phases of several

of these compounds have been measured,[46,47] and it is observed that the tightest packing, and therefore most stable structure, is obtained when adjacent molecules are rotated by 45−60° relative to each other, so that the aromatic cores touch each other but the thicker alkyl chains are not too tightly packed.[48] At the same time, it has often been observed (see, e.g., ref 30) that triphenylenes with a single functionalized polar tail display a mesophase with a lamellar or low-symmetry structure rather than a hexagonal-columnar structure. This presumably arises from a tendency for the polar tails to line up with each other, breaking the 3-fold or cylindrical symmetry of the columns.[49]

In the present case, we may see a competition between the steric repulsion of the tails and their attraction due to hydrogen bonding. In pure **1** or **4**, the tendency toward hydrogen bonding favors a relative rotation angle of 0°, resulting in the sterically unfavorable juxtaposition of the tails. In a mixture of **1** + **4**, a considerable degree of hydrogen bonding can be achieved with a 180° relative rotation of the cores, resulting in a sterically favorable configuration. Thus, the enhanced mesophase range of the bulk **1** + **4** mixture has the same origin as the smaller molecular area at the air−water interface. The **1** + **4** mixture also has a much larger mesophase range than the 69−122 °C mesophase range of the "parent" compound, pure hexapentyloxytriphenylene.[8] This is understandable, since in the latter compound, although the cores can have a large relative rotation, there is no hydrogen bonding.

The photoconductive properties of such films are currently being studied.[49] The photoconductivity of thin films of **1**+ **4** is comparable to those of other triphenylenes forming discotic LB films. It appears to be governed by the same charge generation and transport mechanisms, but differs quantitatively from both **1** and **4**. The time-averaged photoconductivity of these compounds is also under investigation; the stationary photoconductivity of films of **1** + **4** is similar to that of bulk LC systems, showing that the photophysical properties of LB films might be tuned through self-organization of mixtures at the air−water interface.

Acknowledgment. We thank J. K. Blasie for the use of his film balance. We thank Gregory C. Farrington, University of Pennsylvania, and Richard A. Reynolds and Arthur N. Chester, Hughes Research Labs, Malibu, CA, for their support. We acknowledge technical assistance by R. Fischetti and M. Stetzer. Work at the University of Pennsylvania was supported by National Science Foundation grants DMR MRL 92-20668 and DMR 93-15341. Research was carried out in part at the National Synchrotron Light Source (NSLS), Brookhaven National Laboratory, which is supported by the U.S. Department of Energy, Division of Materials Science and Division of Chemical Sciences. NSLS Beamline X9B is supported by the National Institutes of Health under grant No. RR-01633. Work at Mainz was partially supported by a BMFT grant (F&E 13N278) of the German government.

JA964036W

(46) Cotrait, M.; Marsau, P.; Destrade, C.; Malthete, J. *J. Phys. Fr.* **1979**, *40*, L-519.

(47) Heiney, P.; Fontes, E.; de Jeu, W. H.; Riera, A.; Carroll, P.; Smith, A. B., III *J. Phys. Fr.* **1989**, *50*, 461.

(48) Pesquer, M.; Cotrait, M.; Marsau, P.; Volpilhac, V. *J. Phys. Fr.* **1980**, *47*, 351.

(49) Vaes, A., Ph.D. Thesis, Katholieke Universiteit Leuven (KUL), Leuven, Belgium (unpublished).